



## NRC Publications Archive Archives des publications du CNRC

### The preparation and characterization of highly fluorinated poly(arylene alkylene ether)s

Ding, Jianfu; Qi, Yinghua

This publication could be one of several versions: author's original, accepted manuscript or the publisher's version. / La version de cette publication peut être l'une des suivantes : la version prépublication de l'auteur, la version acceptée du manuscrit ou la version de l'éditeur.

For the publisher's version, please access the DOI link below. / Pour consulter la version de l'éditeur, utilisez le lien DOI ci-dessous.

#### **Publisher's version / Version de l'éditeur:**

<https://doi.org/10.1021/ma071669u>

*Macromolecules*, 41, 3, pp. 751-757, 2008

#### **NRC Publications Record / Notice d'Archives des publications de CNRC:**

<https://nrc-publications.canada.ca/eng/view/object/?id=abe1ae11-123c-4495-a545-d20f6b766cd8>

<https://publications-cnrc.canada.ca/fra/voir/objet/?id=abe1ae11-123c-4495-a545-d20f6b766cd8>

Access and use of this website and the material on it are subject to the Terms and Conditions set forth at

<https://nrc-publications.canada.ca/eng/copyright>

READ THESE TERMS AND CONDITIONS CAREFULLY BEFORE USING THIS WEBSITE.

L'accès à ce site Web et l'utilisation de son contenu sont assujettis aux conditions présentées dans le site

<https://publications-cnrc.canada.ca/fra/droits>

LISEZ CES CONDITIONS ATTENTIVEMENT AVANT D'UTILISER CE SITE WEB.

**Questions?** Contact the NRC Publications Archive team at

PublicationsArchive-ArchivesPublications@nrc-cnrc.gc.ca. If you wish to email the authors directly, please see the first page of the publication for their contact information.

**Vous avez des questions?** Nous pouvons vous aider. Pour communiquer directement avec un auteur, consultez la première page de la revue dans laquelle son article a été publié afin de trouver ses coordonnées. Si vous n'arrivez pas à les repérer, communiquez avec nous à PublicationsArchive-ArchivesPublications@nrc-cnrc.gc.ca.



# The Preparation and Characterization of Highly Fluorinated Poly(arylene alkylene ether)s

Jianfu Ding\* and Yinghua Qi

*Institute for Chemical Process and Environmental Technology (ICPET), National Research Council of Canada, 1200 Montreal Road, Ottawa, Ontario, Canada K1A 0R6*

*Received July 26, 2007; Revised Manuscript Received November 20, 2007*

**ABSTRACT:** A series of highly fluorinated poly(arylene alkylene ether)s,  $P6C_FX_s$  ( $X = \text{Non, S, K, SO, Ox}$ ) have been prepared by polycondensation reactions of 1*H*,1*H*,6*H*,6*H*-perfluorohexane-1,6-diol ( $6C_F$ -diol) with a series of decafluorodiphenyl compounds (DFPXs) including decafluorobiphenyl (DFP), decafluorodiphenyl sulfide (DFPS), decafluorobenzophenone (DFPK), decafluorodiphenyl sulfone (DFPSO), and decafluorodiphenyl oxadiazole (DFPOx). This aromatic nucleophilic substitution polycondensation can be effectively activated by cesium fluoride (CsF) and was completed in a few hours in *N,N*-dimethylacetamide (DMAc) at room temperature. High molecular weight polymers ( $M_n = 28\,200\text{--}64\,200$  Da) have been prepared from DFP, DFPS, DFPSO, and DFPOx, while the reaction from DFPK only yields low-molecular weight materials ( $M_n < 8\,000$  Da). A model reaction using excess  $6C_F$ -diol (2.5 equiv of DFPK) reveals that the ketone linkage of the DFPK unit is cleaved by the attack of the activated hydroxyl group in the diol during the polycondensation. This cleavage is suppressed when potassium fluoride (KF) was used as a base, and a high molecular weight  $P6C_FK$  ( $M_n = 33\,200$  Da) has been prepared. DSC analysis shows that all the resultant polymers are semicrystalline materials, and the melted samples display different crystallization rates in the order of  $P6C_F\text{Non} > P6C_F\text{Ox} > P6C_FK > P6C_F\text{SO} \sim P6C_FS$ . This sequence is correlated with the bond angles of the X linkages, suggesting a significant influence of the bending of the X linkages on the crystallization capability of the polymers. The  $P6C_F\text{Non}$  film has a hydrophobic surface with a water contact angle of  $110^\circ$ , while the other polymers showed reduced values with the increase of the polarities of the X linkages in the order of  $P6C_F\text{Non} > P6C_FS > P6C_FK > P6C_F\text{Ox} > P6C_F\text{SO}$ .

## Introduction

Highly fluorinated polymers such as polytetrafluoroethylene (Teflon) are very attractive in many applications, because of their excellent electronic and optical properties, high thermal and chemical stabilities, and special surface properties associated with their very low surface tension.<sup>1</sup> However, fully fluorinated polymers such as Teflon usually have a very poor processability and thus their applications are restricted. Therefore many partially fluorinated polymers with improved processability have been studied.<sup>1b,d</sup> Among them, fluorinated poly(arylene ether)s exhibited a great potential of achieving high fluorine content and attracted much attention for optical and electronic applications such as optical waveguide devices, low surface energy coatings, and so on.<sup>1,2</sup>

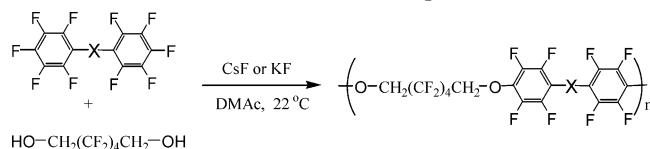
However, the fluorine content in the fluorinated poly(arylene ether)s are still limited to a moderate level due to the low fluorine content of the bisphenol monomers used for the preparation of the polymers.<sup>3–5</sup> Bisphenols with fluorine atoms attached to the phenyl ring are not stable; consequently the fluorine contents of these monomers are limited. Alternatively, replacing the bisphenols with highly fluorinated diols in this reaction could be a promising approach to obtain polyethers with high fluorine contents.<sup>6,7</sup> The produced polymers consist of asymmetrical ether bonds with an aromatic and an aliphatic segment at both sides. Because of the high fluorine content, like Teflon, these fluorinated poly(arylene alkylene ether)s are expected to have low surface tensions, low refractive indices, low glass transition temperatures, and low optical losses in the optical communication wavelength region. Furthermore, because of the existence of the ether and the other functional groups,

these polymers will have a better processability, in addition to an increased flexibility in chemical structure modification to achieve specific properties.

Only limited work related to these polymers has been reported due to difficulties in the polymer preparation.<sup>6,7</sup> As mentioned above, the nucleophilic polycondensation of a DFPX with a fluorinated alkylene diol is considered the most promising technique for the polymer preparation. In this reaction, the alkoxide anion formed from the diol by interacting with a base is a stronger nucleophile than the phenoxide anion in the reaction for the preparation of the poly(arylene ether)s, consequently it is more reactive to attack the para positions for the formation of the desired linear polymer structure as well as the ortho positions of DFPX for the formation of branched and crosslinked structures. Moreover, this branching side reaction will break the stoichiometric balance between para fluorines and OH groups and prevent the formation of high-molecular weight polymers. As a result, from a series of DFPXs, only DFP has been reported for successfully polymerizing with a fluorinated diol to give high-molecular weight polymers.<sup>7</sup> In this case, the polymerization is probably benefited from the specific structure of DFP, in which the four ortho fluorine atoms overlap due to the short distance between the adjacent phenyl rings to create significant steric hindrance for the side reaction at these four ortho positions. When other DFPXs with a X linkage inserted between the phenyl rings such as DFPK were used, the ortho fluorine atoms on the adjacent phenyl rings of the monomers do not overlap anymore and the side reaction at these ortho positions becomes more likely; consequently, only low-molecular weight polymers ( $M_n = 5\,200$  Da for the ketone polymer) could be produced.<sup>7</sup>

Recently we found that cesium fluoride (CsF) or potassium fluoride (KF) is a sufficiently strong base to activate the

\* To whom correspondence should be addressed. E-mail: jianfu.ding@nrc-cnrc.gc.ca.

Scheme 1. Reaction Route for the Preparation of P6C<sub>F</sub>Xs

X	none	—S—			
Polymer	P6C <sub>F</sub> Non	P6C <sub>F</sub> S	P6C <sub>F</sub> K	P6C <sub>F</sub> SO	P6C <sub>F</sub> Ox

fluorinated alkylene diol to react with DFPSO in DMAc at room temperature to produce high-molecular weight polymers. Furthermore, they appeared sufficiently mild to suppress the side reaction at the ortho positions of DFPSO.<sup>8</sup> In the present article, we extend this reaction to other DFPXs with different X linkages including Non, sulfide, ketone, and oxadiazole as illustrated in Scheme 1.

### Experimental Section

**Materials.** 1*H*,1*H*,6*H*,6*H*-perfluoro-1,6-hexanediol (6C<sub>F</sub>-diol) was purchased from Oakwood Products Inc. and used as received. Decafluorobiphenyl (DFP), decafluorobenzophenone (DFPK), anhydrous DMAc, and all other chemicals were obtained from Sigma-Aldrich, DFP and DFPK were purified by recrystallization from 2-propanol prior to use. Decafluorodiphenyl oxadiazole (DFPOx), decafluorodiphenyl sulfide (DFPS), and decafluorodiphenyl sulfone (DPSO) were prepared according to reported methods.<sup>5a,e</sup>

**Characterizations.** Nuclear magnetic resonance (NMR) spectra were recorded using a Varian Unity Inova spectrometer at a resonance frequency of 400 MHz for <sup>1</sup>H NMR and 376 MHz for <sup>19</sup>F NMR in acetone-*d*<sub>6</sub>. Aliquots of 0.05 mL were taken from the reaction solution at different reaction times and were directly added into acetone-*d*<sub>6</sub> for kinetics study, while purified polymers were used for structural analysis. The chemical shifts relative to tetramethylsilane for <sup>1</sup>H NMR and CFCl<sub>3</sub> for <sup>19</sup>F NMR are reported on the ppm scale. The molecular weights of the polymers were determined by size exclusion chromatography (SEC) using a Viscotek SEC system, which consists of a Viscotek VE1122 HPLC pump coupled with a Viscotek TDA triple detector and a Viscotek 2501 UV detector operated at 260 nm. A set of ViscoGEL columns (G4000H and G5000H) was used and calibrated by a set of polystyrene standards in THF. The flow rate is 1 mL/min, and the columns and the detectors were operated at 35 °C. IR spectra were recorded with a Midac M1200-SP3 spectrophotometer using a diamond cell. Differential scanning calorimetric (DSC) measurements and thermogravimetric analyses (TGA) were performed on a TA Instruments DSC 2920 and on a TA Instruments TGA 2950, respectively, using a heating rate of 10 °C/min under nitrogen. Contact angles of the polymer films on glass slides were measured with a FTA200 dynamic contact angle analyzer from Folio Instruments Inc. The samples were prepared by spin coating a 5% THF solution on glass slides at 2000 rpm. The films were baked in a 100 °C oven for 2 h prior to the water contact angle measurement. The reported data is the average value of five measurements at different spots of a sample.

**Synthesis of P6C<sub>F</sub>Ox from DFPOx and 6C<sub>F</sub>-Diol.** To a solution of DFPOx (0.8084 g, 2.01 mmol) and 6C<sub>F</sub>-diol (0.5242 g, 2.00 mmol) in anhydrous DMAc (8 mL) was added CsF (0.91 g, 6.0 mmol). The mixture was stirred at room temperature for 2.5 h. After filtration to remove inorganic solids, the polymer solution was added dropwise into methanol (200 mL) with agitation. The resulting fibrous white polymer was collected by filtration, washed thoroughly with methanol, and dried at room temperature under vacuum for 12 h. (1.04 g, 83% yield). <sup>1</sup>H NMR (400 MHz, acetone-*d*<sub>6</sub>): δ (ppm) 5.217 (t, *J* = 13.4 Hz). <sup>19</sup>F NMR (376 MHz, acetone-*d*<sub>6</sub>): δ (-121.80 (4F, m), -124.32 (4F, m), -139.24 (4F, m), -156.86 (4F, m). IR (cm<sup>-1</sup>): 2974 (CH stretching), 1653, 1562, 1515, 1484

Table 1. The Preparation and Characterization of the Polymers

polymer	time <sup>a</sup> (h)	M <sub>n</sub> <sup>c</sup> (kDa)	PDI	T <sub>g</sub> <sup>d</sup> (°C)	T <sub>m</sub> <sup>e</sup> (°C)	ΔH <sup>d</sup> (J/g)	T <sub>d</sub> <sup>5%</sup> <sup>f</sup> (°C)	Ψ (deg) <sup>g</sup>
P6C <sub>F</sub> Non	1.0	49.4	2.7	26	219	18.3	384	110
P6C <sub>F</sub> S	7.0	64.2	4.2	25	121	12.5	402	109
P6C <sub>F</sub> K	21 <sup>b</sup>	33.2	3.6	22	165	18.6	396	102
P6C <sub>F</sub> SO	4.0	44.0	6.5	87	174	10.6	415	82
P6C <sub>F</sub> Ox	2.5	28.2	3.7	45	202	21.3	396	95

<sup>a</sup> The polycondensation was conducted in DMAc in the presence of CsF at 22 °C. <sup>b</sup> The preparation of P6C<sub>F</sub>K was conducted in DMAc in the presence of KF at 22 °C. <sup>c</sup> M<sub>n</sub> and PDI values were obtained from SEC measurement. <sup>d</sup> T<sub>g</sub> value was measured from the second heating scan; the sample was quenched from 250 °C by immersing the samples into liquid nitrogen to make the glass transition detectable. <sup>e</sup> T<sub>m</sub> and ΔH were derived from the first heating scan curve of the DSC measurement. <sup>f</sup> T<sub>d</sub><sup>5%</sup> was detected using TGA under the protection of nitrogen. <sup>g</sup> Contact angle, the experimental error is 5°.

(phenyl ring), 1210, 1176, 1116 (ether), 996, 843, 725, 543. T<sub>g</sub>: 45 °C. T<sub>m</sub>: 202 °C. M<sub>n</sub>: 28 200 Da. M<sub>w</sub>/M<sub>n</sub>: 3.7.

**Synthesis of P6C<sub>F</sub>SO, P6C<sub>F</sub>S, and P6C<sub>F</sub>Non.** These polymers were prepared from the corresponding decafluorodiphenyl monomers and 6C<sub>F</sub>-diol with a feed ratio of [DFPX]/[6CF-diol] = 2.01/2.00 using the same procedure as described above with the reaction time listed in Table 1 and the characterization as the following.

**P6C<sub>F</sub>SO.** (90% yield). <sup>1</sup>H NMR (400 MHz, acetone-*d*<sub>6</sub>), δ (ppm): 5.201 (t, *J* = 13.2 Hz). <sup>19</sup>F NMR (376 MHz, acetone-*d*<sub>6</sub>), δ (ppm): -121.87 (4F, m), -124.33 (4F, m), -139.88 (4F, m), -155.81 (4F, m). IR (cm<sup>-1</sup>): 2982 (CH stretching), 1638, 1500 (phenyl ring), 1391, 1177, 1128 (ether), 1013, 990, 659, 583, 559. T<sub>g</sub>: 87 °C. T<sub>m</sub>: 174 °C. M<sub>n</sub>: 44 000 Da. M<sub>w</sub>/M<sub>n</sub>: 6.5.

**P6C<sub>F</sub>Non.** (88% yield). <sup>1</sup>H NMR (400 MHz, acetone-*d*<sub>6</sub>), δ (ppm): 5.167 (t, *J* = 13.6 Hz). <sup>19</sup>F NMR (376 MHz, acetone-*d*<sub>6</sub>), δ (-121.88 (4F, m), -124.35 (4F, m), -141.28 (4F, m), -157.16 (4F, m). IR (cm<sup>-1</sup>): 2966 (CH stretching), 1651, 1596, 1499 (phenyl ring), 1401, 1285, 1180, 1115 (ether), 987, 872, 727, 533. T<sub>g</sub>: 26 °C. T<sub>m</sub>: 219 °C. M<sub>n</sub>: 49 400. M<sub>w</sub>/M<sub>n</sub>: 2.7.

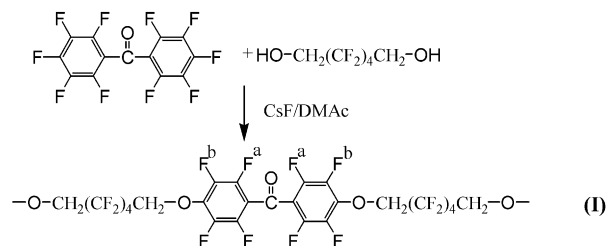
**P6C<sub>F</sub>S.** (86% yield). <sup>1</sup>H NMR (400 MHz, acetone-*d*<sub>6</sub>), δ (ppm): 5.052 (t, *J* = 13.6 Hz). <sup>19</sup>F NMR (376 MHz, acetone-*d*<sub>6</sub>), δ (-121.93 (4F, m), -124.39 (4F, m), -135.75 (4F, m), -156.87 (4F, m). IR (cm<sup>-1</sup>): 2980 (CH stretching), 1634, 1499 (phenyl ring), 1491, 1292, 1155, 1120 (ether), 988, 872, 765, 732, 661, 596, 559. T<sub>g</sub>: 25 °C. T<sub>m</sub>: 121 °C. M<sub>n</sub>: 64 200. M<sub>w</sub>/M<sub>n</sub>: 4.2.

**Synthesis of P6C<sub>F</sub>K from DFBP and 6C<sub>F</sub>-Diol.** To a solution of DFBP (0.7314 g, 2.02 mmol) and 6C<sub>F</sub>-diol (0.5243 g, 2.00 mmol) in anhydrous DMAc (8 mL) was added potassium fluoride (0.35 g, 6.0 mmol). The mixture was stirred at 22 °C for 21 h. The reaction mixture was centrifuged, and the supernatant was added dropwise into methanol (200 mL) with agitation. The resulting fibrous white polymer was collected by filtration, washed thoroughly with methanol, and dried at room temperature under vacuum for 12 h. (1.01 g, 86% yield). <sup>1</sup>H NMR (400 MHz, acetone-*d*<sub>6</sub>): δ 5.196 (t, *J* = 13.4 Hz). <sup>19</sup>F NMR (376 MHz, acetone-*d*<sub>6</sub>): δ (-121.86 (4F, m), -124.35 (4F, m), -144.82 (4F, m), -156.92 (4F, m). IR (cm<sup>-1</sup>): 2974 (CH stretching), 1752, 1696, 1649, 1490 (phenyl ring), 1408, 1329, 1174, 1123 (ether), 991, 777, 736, 674, 535. T<sub>g</sub>: 22 °C. T<sub>m</sub>: 165 °C. M<sub>n</sub>: 33 200 Da. M<sub>w</sub>/M<sub>n</sub>: 3.6.

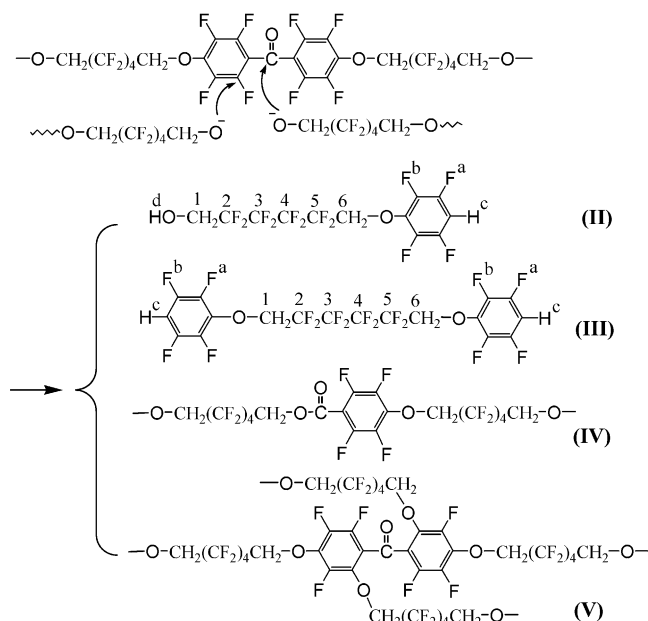
**Model Reaction of DFBP (1.00 Equivalents) and 6C<sub>F</sub>-Diol ((2.5 Equivalents).** To a solution of DFBP (0.3618 g, 1.00 mmol) and 6C<sub>F</sub>-diol (0.6553 g, 2.50 mmol) in anhydrous DMAc (8 mL) was added CsF (0.61 g, 4.0 mmol). Aliquots of 0.05 mL of the reaction solution were taken at selected reaction times and were filtered to remove solids and then dropped into 0.5 mL of acetone-*d*<sub>6</sub> for <sup>1</sup>H and <sup>19</sup>F NMR analysis. The final reaction solution at 400 min was centrifuged and part of the supernatant was dropped into methanol/water (1/9, v/v) mixture. The resulting white powder was collected by centrifuge, washed with water twice, and dried at room temperature under vacuum for 12 h. The obtained powder represents the whole reaction product containing several compounds as listed in Scheme 2 and was characterized by FT-IR, IR (cm<sup>-1</sup>): 2974 (CH stretching), 1751, 1686, 1633 1481 (phenyl ring), 1400, 1322,

**Scheme 2. Possible Reaction of DFBP (1.0 Equivalent) with Excess 6C<sub>F</sub>-diol (2.5 Equivalent) in DMAc in the Presence of CsF at Room Temperature**

1<sup>st</sup> Step: Substitution at para-positions:



2<sup>nd</sup> Step: Ketone cleave and/or substitution at ortho-positions:



1162, 1123 (ether), 1058, 956, 871, 779, 723, 561. Meanwhile, 1 mL of the supernatant was also dropped into 10 mL of hexane and agitated at room temperature for 5 min for extracting the soluble part of the product. The top layer was separated and evacuated to remove the solvent. This hexane extracted sample was characterized by <sup>1</sup>H and <sup>19</sup>F NMR. <sup>1</sup>H NMR (400 MHz, acetone-*d*<sub>6</sub>): δ (ppm) 7.23 (m), 4.95 (t, *J* = 6.2 Hz), 4.82 (t, *J* = 14.0 Hz), 3.96 (t, *J* = 14.9 Hz). <sup>19</sup>F NMR (376 MHz, acetone-*d*<sub>6</sub>): δ (ppm) -122.09, -123.01, -124.41, -124.61, -124.76, -141.70, -158.13.

## Results and Discussion

**The Polycondensation of DFPXs with 6C<sub>F</sub>-Diol.** The decafluorodiphenyl monomers (DFPXs) studied in this work have a general formula as illustrated in Scheme 1. The X linkages in these compounds are Non for decafluorobiphenyl (DFP), sulfide for decafluorodiphenyl sulfide (DFPS), ketone for decafluorobenzophenone (DFPK), sulfone for decafluorodiphenyl sulfone (DFPSO), and oxadiazole for decafluorodiphenyl oxadiazole (DFPOx). As reported in our previous work,<sup>8</sup> the polycondensation between DFPSO and 6C<sub>F</sub>-diol can be easily completed in DMAc at room temperature with CsF as a base. With the exception of DFPK, the other DFPXs also have a reasonable reactivity under this reaction condition and give high-molecular weight polymers. As usually found in a conventional polycondensation of DFPX monomers,<sup>3-5</sup> a side reaction at the ortho position of DFPXs is possible in this reaction. This side reaction will result in branching and

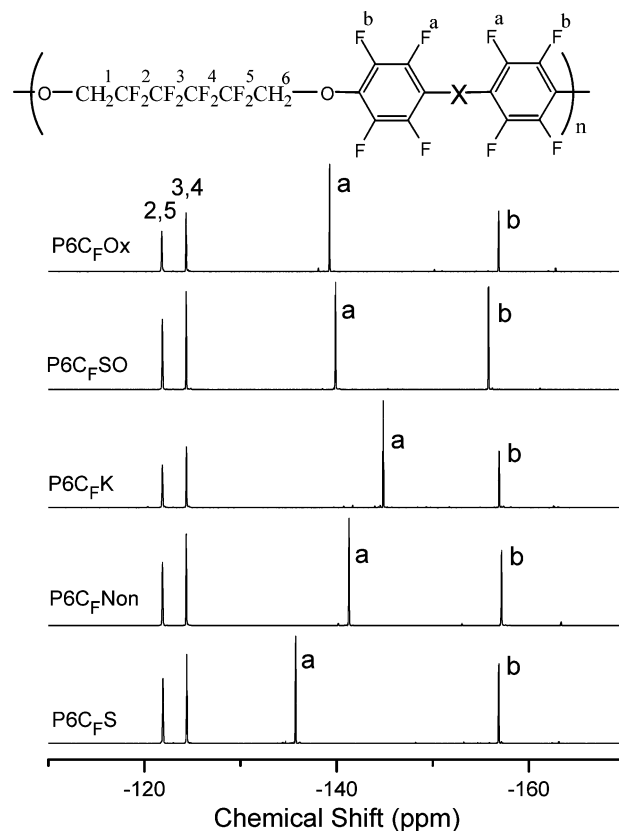


**Figure 1.** <sup>19</sup>F NMR spectra of the purified samples of P6C<sub>F</sub>Xs in acetone-*d*<sub>6</sub>.

eventually cross-linking of the polymer and produce corresponding peaks in <sup>19</sup>F NMR.<sup>4c-f</sup> Figure 1 displays that the produced polymers have clean <sup>19</sup>F NMR spectra. Besides the four major peaks assigned to the fluorine atoms on the main chain as indicated in the figure, only three tiny peaks, which are almost immersed into the background, can be seen. They correspond to the para, ortho, and meta fluorine atoms on the end group. No other resonance with comparable intensity is observable. This result indicates that the branching reaction is strongly suppressed under this reaction condition. This is believed to be due to the low reaction temperature. Actually the reactions at a higher temperature (60 °C) of the reactive monomers such as DFPSO could yield crosslinked gels. A similar conclusion is also drawn from the <sup>1</sup>H NMR studies that show only one triplet around 5.2 ppm, which is ascribed to the 1 and 6 protons of the 6C<sub>F</sub>-diol units. The chemical shift of the peak slightly moves to downfield with the increasing polarity of the X linkage in the DFPX units with the values (in ppm) of 5.052 for P6C<sub>F</sub>S, 5.167 for P6C<sub>F</sub>Non, 5.196 for P6C<sub>F</sub>K, 5.201 for P6C<sub>F</sub>SO, and 5.217 for P6C<sub>F</sub>Ox.

SEC data in Table 1 reveals that all polymers have a large *M<sub>w</sub>/M<sub>n</sub>* value, which is much higher than that from a typical polycondensation reaction. As explained in our previous work,<sup>8</sup> the high-molecular weight distribution should be attributed to the heterogeneous reaction condition. In this reaction, the base existed in solution mostly as solid particles. The adsorption of the polymer on the particle surface will act as a barrier layer and cause a higher base concentration and a higher propagation rate of the polymers near the solid surface than in the solution. This effect broadens the molecular weight distribution, especially when molecular weight of the polymer is getting high.

**Side Reactions Occurring during the Polycondensation of DFPK with 6C<sub>F</sub>-Diol.** DFPK displays a different behavior with

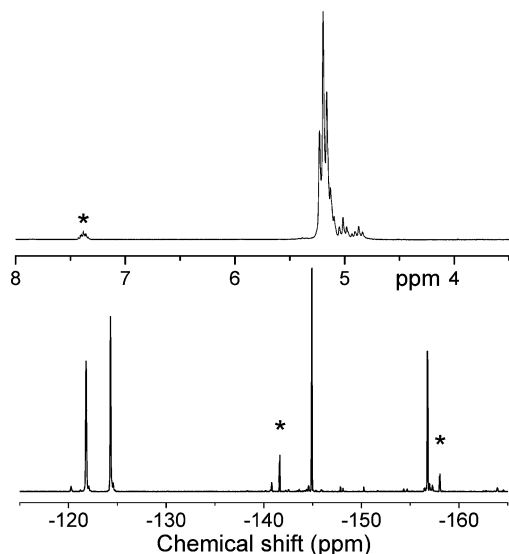


**Figure 2.**  $^1\text{H}$  (top) and  $^{19}\text{F}$  (bottom) NMR spectra of the final reaction solution of the polycondensation between DFPK and  $6\text{C}_\text{F}$ -diol in DMAc using CsF as a base.

the other monomers in the polycondensation with  $6\text{C}_\text{F}$ -diol in the presence of CsF, which only produce polymers with  $M_n$  lower than 8 000 Da.  $^1\text{H}$  and  $^{19}\text{F}$  NMR analysis revealed some unexpected peaks in the spectra of the resulting polymer, which were marked with stars in Figure 2, indicating side reactions occurred during the polycondensation. Previous works show that the ketone group in benzophenone is sensitive to the nucleophilic attack by  $\text{HO}^-$  or  $\text{RO}^-$  and can be cleaved to form benzoic acid and benzene moieties.<sup>5c,9</sup> This fact suggests that a similar cleavage might also occur during the polycondensation to cause the degradation of the produced polymer. The strong electron-withdrawing effect of the multiple fluorine on the phenyl ring adjacent to the ketone group will further promote this side reaction<sup>10</sup> and makes this cleavage occur under a milder reaction condition such as in the presence of potassium fluoride.<sup>5c</sup> Therefore, we believe the small peaks found at  $-141.6$  and  $-158.0$  ppm in the  $^{19}\text{F}$  NMR spectrum and at  $7.43$  and  $5.01$  ppm in the  $^1\text{H}$  NMR spectrum (see Figure 2) are related to the moieties resulting from the ketone cleavage with the possible structures listed in Scheme 2 (compounds II–IV).

To further investigate this side reaction, a model reaction of DFPK and  $6\text{C}_\text{F}$ -diol under the same condition as the polymerization was studied using excess  $6\text{C}_\text{F}$ -diol (2.5 equiv to DFPK).  $^{19}\text{F}$  NMR was used to monitor the reaction with the representative spectra displayed in Figure 3. They reveal that the reaction in the first few minutes is clean; only the reaction of the hydroxyl group of the diol at the para positions of DFPK is observed. This reaction is fast and completed in 4 min to form the structure I as illustrated in Scheme 2. At this time, only two resonances were found at  $-144.9$  (Ia) and  $-156.9$  (Ib) ppm for the aromatic fluorine atoms, and four peaks were observed for the four fluorine atoms on the third and fourth carbons of the diol unit at  $-121.82$ ,  $-122.01$ ,  $-122.83$ , and  $-123.03$  ppm and also another four peaks for those on the second and fifth carbons at  $-124.32$ ,  $-124.56$ ,  $-124.69$ , and  $-124.88$  ppm. Among them, the peaks at  $-123.03$  and  $124.88$  ppm are ascribed to the unreacted diol, the peaks at  $-122.01$ ,  $-122.83$ ,  $-124.56$ , and  $-124.69$  come from the diol unit with one substituted end, and those at  $-121.82$  and  $-122.01$  are from the diol unit with both substituted ends. From the integration of these peaks, it can be estimated that 37.4% of the diol remains untouched, about 45.8% of them with one substituted end and 16.8% with

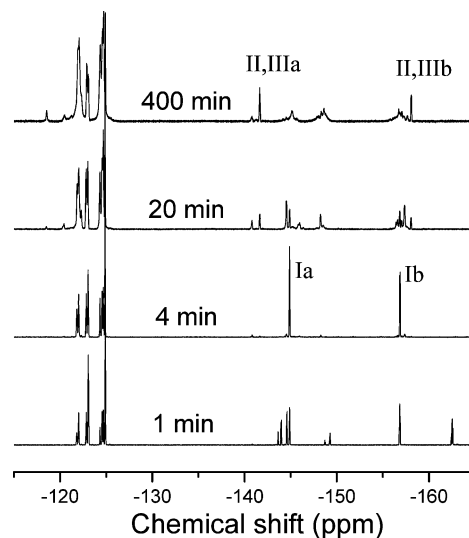


**Figure 3.**  $^{19}\text{F}$  NMR spectra of the solution taken at different times from the reaction of DFBP (1.0 equiv) with  $6\text{C}_\text{F}$ -diol (2.5 equiv) in DMAc using CsF as a base. A 0.05 mL aliquot taken from the reaction solution was directly added into 0.5 mL of acetone- $d_6$  for NMR analysis. (See Scheme 2 for the peak assignment.)

both ends substituted. After this time, the further reaction reduces the intensity of these two aromatic peaks and finally leads to the formation of two new sharp peaks at  $-141.7$  and  $-158.1$  ppm and three broad peaks at  $-145.1$ ,  $-148.7$ , and  $-157.0$  ppm for the final reaction solution at 400 min. These three broad peaks have similar integral intensities, and a prediction by ACD software indicates that they are related to the product of the substitution of the first ortho fluorine of each phenyl ring in the DFPK unit with a structure represented by compound V in Scheme 2. Because the molar ratio of  $6\text{C}_\text{F}$ -diol/DFPK is 2.5, a fraction of the second hydroxyl group of the  $6\text{C}_\text{F}$ -diol unit is involved in the reaction (also see above discussion on the 4 min NMR spectrum of Figure 3), which produced a densely branched structure in the product. It might explain that the corresponding peaks are very wide. On the other hand, the two narrow peaks may indicate that they are associated with small molecules which can move freely in the solution. To verify this assumption, the final solution of this reaction was extracted with hexanes in order to separate the free molecules, and the extracted material was found to be a mixture of compounds II and III by  $^1\text{H}$  and  $^{19}\text{F}$  NMR analysis. The resonances assigned in Figure 4 use the structures shown in Scheme 2. Therefore, we can conclude that the sharp peaks in the spectrum of the 400 min sample in Figure 3 and the peaks indicated with stars in Figure 2 are due to the formation of tetrafluorobenzene moieties, resulting from the ketone cleavage. It should be noted that the solution for collecting spectra in Figure 2 contains small amounts of DMAc from the reaction solution, while the solution for Figure 4 does not. This causes slight differences in the chemical shifts of certain peaks between Figures 2 and 4.

The above NMR study only reveals the phenyl product from the benzophenone cleavage. The counterpart of the cleaving products, benzoate (compound IV), is not observed in the hexane extracted sample. Compared to compounds II and III, compound IV contains one more  $6\text{C}_\text{F}$ -diol unit, in addition to a carbonyl activated tetrafluorophenyl ring. Both the hydroxyl groups in the  $6\text{C}_\text{F}$ -diol units and the ortho fluorines in the tetrafluorophenyl ring can participate further in the branching side reaction to form large molecules. Therefore, this part of the cleaved product is less likely to be isolated from the other materials by hexane

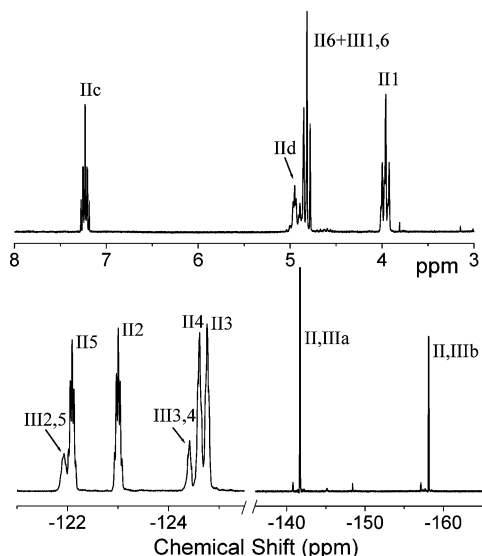


**Figure 4.**  $^1\text{H}$  (top) and  $^{19}\text{F}$  (bottom) NMR spectra of the sample extracted using hexane from the final solution (400 min) of the reaction between DFBP (1.0 equiv) with  $6\text{C}_\text{F}_2$ -diol (2.5 equiv) in DMAc using CsF as a base.

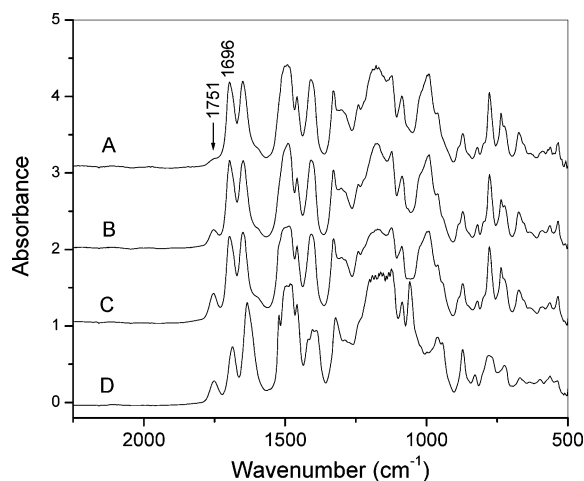


**Figure 5.** FT-IR spectra of the final samples from the reactions of DFBP with  $6\text{C}_\text{F}_2$ -diol with the molar ratio of 1.01/1.00 (A) in the presence of CsF in PC, (B) in the presence of KF in DMAc, (C) in the presence of CsF in DMAc, and (D) with the molar ratio of 1.00/2.50 in the presence of CsF in DMAc.

extraction. The FT-IR spectrum of the purified whole product of this reaction (Figure 5D) displayed a moderate peak at  $1751\text{ cm}^{-1}$ , which is assigned to the stretching of the ester carbonyl  $\text{C}=\text{O}$  bond, while the intensity of the ketone stretching at  $1696\text{ cm}^{-1}$  is decreased relative to the other peaks. This result confirms part of the ketone group was cleaved to the carbonyl ester group during the reaction.

In conclusion, there are two side reactions to compete with the polycondensation at the para positions for the formation of the linear polymer. One is the ketone cleavage, and the other is the substitution at the ortho positions of the DFBP unit. The former will reduce the molecular weight of the produced polymer, and the latter will lead to the formation of branched structures. From the  $^{19}\text{F}$  NMR analysis (Figure 3), the conversion of these three reactions can be calculated based on the intensities of the corresponding peaks and the results are displayed in Figure 6. It clearly indicates that the two side reactions have relatively low reaction rates and only occur after the polycondensation at the para positions is near completion. When the conversion of the polycondensation reaches 99%, the conversion

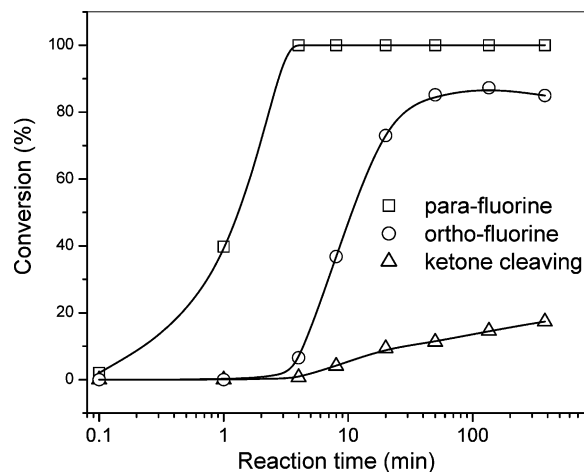


**Figure 6.** Time dependence of the conversions of the substitution of the para-fluorines, the substitution of the first ortho fluorine on each phenyl ring in DFBP units, and the ketone cleavage in the reaction of DFBP (1.00 equiv) with  $6\text{C}_\text{F}_2$ -diol (2.50 equiv) in the presence of CsF in DMAc at room temperature as illustrated in Scheme 2.

for the ketone cleavage is only about 1%. This suggests that a high-molecular weight polymer can be prepared in this reaction provided the polycondensation can be controlled well. However, due to the very high reaction rates of both polycondensation and the side reactions, precise control this reaction is practically almost impossible.

**The Preparation of  $\text{P6C}_\text{F}_7\text{K}$  Using KF as a Base.** Therefore, some milder reaction conditions have been tested to achieve a better control of the reaction. Among them, the reaction in the presence of KF as a base in DMAc at room-temperature gave the highest molecular weight ( $M_n = 33\,200\text{ Da}$ ) of the resulting polymers. The FT-IR spectrum of this polymer is compared with the materials prepared under other conditions in Figure 5. It shows a much smaller carbonyl stretching peak at  $1751\text{ cm}^{-1}$ , indicating a much lower tendency of the ketone cleavage. Figure 5 also showed that the reaction in propylene carbonate by the use of CsF as a base at room temperature can further suppress this ketone cleavage. However, the polymer prepared under this condition is difficult to dissolve, probably associated with the formation of a highly branched structure. Consequently,  $\text{P6C}_\text{F}_7\text{K}$  has been prepared using KF in DMAc at room temperature and the reaction is completed in 21 h.

**Thermal Properties of  $\text{P6C}_\text{F}_7\text{Xs}$ .** DSC study revealed that all polymers are semicrystalline materials. The first heating curves in Figure 7 show a narrow melting peak at 219, 202, and  $165\text{ }^\circ\text{C}$  for  $\text{P6C}_\text{F}_7\text{Non}$ ,  $\text{P6C}_\text{F}_7\text{Ox}$ ,  $\text{P6C}_\text{F}_7\text{K}$ , while  $\text{P6C}_\text{F}_7\text{SO}$  and  $\text{P6C}_\text{F}_7\text{S}$  display a broad melting peak at around 174 and  $121\text{ }^\circ\text{C}$ , respectively. No apparent glass transition was observed for the polymers in the first heating scan. To study the glass transition, the polymer samples were quenched into liquid nitrogen immediately after the first heating scan at  $250\text{ }^\circ\text{C}$ . The DSC curves of these samples are displayed in Figure 8. It can be seen that  $\text{P6C}_\text{F}_7\text{Non}$  still has a melting peak with a very weak glass transition at  $26\text{ }^\circ\text{C}$ , showing that the crystallization of this polymer was completed in the very short quenching period, indicating an extremely high crystallization rate. This should be attributed to the highly symmetric chain structure of this polymer.  $\text{P6C}_\text{F}_7\text{Ox}$  showed a slightly lower crystallization rate than that of  $\text{P6C}_\text{F}_7\text{Non}$ . This polymer displayed a small glass transition at  $45\text{ }^\circ\text{C}$ , immediately followed by a small exothermic peak. This phenomenon indicates that the amorphous domain frozen from the melted state by the rapid quenching can crystallize quickly once the chain segments are capable of

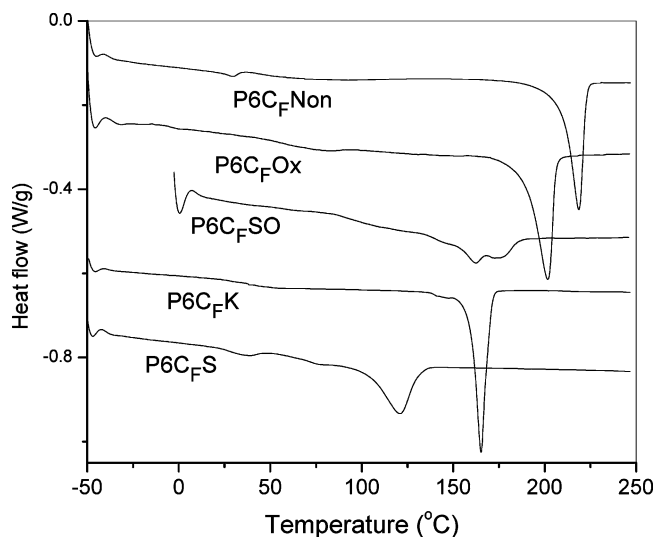


**Figure 7.** DSC curves of the first heating scan of the as-prepared samples of P6C<sub>F</sub>Xs.

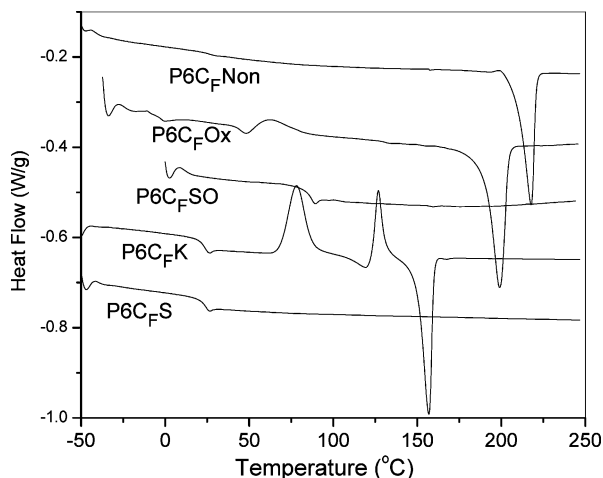


**Figure 8.** DSC curves of the second heating scan after the samples of P6C<sub>F</sub>Xs were quenched into liquid nitrogen from 250 °C.

moving. The quenched samples of the other three polymers with ketone, sulfone, and sulfide linkages display well-resolved glass transitions at 22, 87, and 25 °C, respectively. While the sulfone and sulfide polymers did not show any first-order transition in the second heating scan, the ketone polymer displays two crystallization peaks at 78.5 and 126.7 °C prior to the melting peak with a similar amount of the exothermic and endothermic heats. This indicates that the ketone polymer is completely amorphous after quenching as are the sulfone and sulfide polymers, but the ketone polymer has a higher crystallization rate and crystallizes during the second heating scan at a rate of 10 °C/min. Therefore, we conclude that the crystallization rate is in the order: P6C<sub>F</sub>Non > P6C<sub>F</sub>Ox > P6C<sub>F</sub>K > P6C<sub>F</sub>SO ~ P6C<sub>F</sub>S. This sequence correlates with the bond angles of the X linkages, which are 180° for Non, 134° for oxadiazole, 122° for ketone, 104° for sulfone, and 104° for sulfide.<sup>11</sup> This result evidences that the bending of the X linkages significantly affects the crystallization capability of the polymers.

Meanwhile, the DSC data showed that all the polymers have a very low glass transition temperature ( $T_g$ ) at around 25 °C. This unusual low  $T_g$  might indicate some extent of phase separation in the quenched samples, where aliphatic chain enriched amorphous domains were formed. The  $T_g$  values of the polymers with sulfone and oxadiazole linkages are slightly higher, reflecting high molecular interactions in the polymers

with the more polar groups of sulfone and oxadiazole. Table 1 also lists the degradation temperatures of the polymers. They range from 380 to 415 °C, indicating a fairly high thermal stability of the polymers. However, these values are lower than those of the corresponding fluorinated poly(arylene ether)s,<sup>5</sup> indicating the polymers with asymmetric ether linkages have a slightly poorer thermal stability than the polymers with a symmetric aromatic ether linkage. It is worthy to note that the ketone polymer has a similar degradation temperature as the other polymers, although this polymer is much less stable under the polycondensation condition in the presence of a base in a highly polar solvent as discussed above.

**Water Contact Angles of P6C<sub>F</sub>Xs.** The surface tension of the polymer films has been characterized by water contact angle measurements, and the results are listed in Table 1. The films were coated on glass slides from tetrahydrofuran solutions. Among all the polymers, P6C<sub>F</sub>Non exhibits the highest value of the contact angle of 110°. This value is very close to that of Teflon type materials (112°),<sup>12</sup> the polymers with lowest surface energy. With increasing polarity of the X linkages from sulfide, ketone, oxadiazole, to sulfone, the water contact angle of the corresponding polymer films decreased from 109, 102, 95, to 82°. As expected, the contact angles of these fluorinated polymers are much higher than those of the corresponding non-fluorinated poly(arylene ether)s and also about 10° higher than the partially fluorinated poly(arylene ether)s,<sup>12c,d</sup> confirming the significance of a high fluorine content in the polymer for reducing the surface tension of the polymer films.<sup>1c</sup> A similar phenomenon was also reported for aromatic block copolyethers with amphiphilic structures.<sup>4d</sup> Further investigation of factors including molecular weight, enrichment of fluorine atoms on the surface to influence the contact angle, and the superhydrophobic phenomenon associated with the lotus-leaf-type surface structures is under way.<sup>13</sup>

## Conclusions

When CsF was used as a base to activate the reaction, the polycondensations of 6C<sub>F</sub>-diol with DFP, DFPS, DFPSO, and DFPOx can be easily completed under an extremely mild reaction condition, i.e., a few hours at room temperature in DMAc, to produce high-molecular weight polymers. This mild reaction condition efficiently prevents the side reactions which were usually observed in conventional polycondensations such as ether cleavage and branching. However, the reaction of 6C<sub>F</sub>-diol with DFPK under the same reaction condition only produces a low-molecular weight material. <sup>1</sup>H and <sup>19</sup>F NMR studies reveal the formation of a 4*H*-perfluorophenyl group and a perfluorobenzoate group during the reaction; these moieties are produced from a ketone cleavage side reaction, where the hydroxyl group of 6C<sub>F</sub>-diol which was highly activated by CsF attacks the ketone group in DFPK unit to break the polymer chain. Fortunately, a kinetic analysis has revealed that the ketone cleavage has a much lower reaction rate than the polycondensation, suggesting that a high-molecular weight polymer can be prepared by careful control of the reaction. Therefore, a milder base, KF, instead of CsF has been used for this reaction to give an ideal result. In this case, the polycondensation is completed in 21 h to yield a polymer with  $M_n = 33\,200$  Da.

All the prepared polymers are semicrystalline materials with melting points in the range from 120 to 218 °C. Owing to the different X linkages, different polymers exhibit different crystallization capabilities. P6C<sub>F</sub>Non crystallizes completely during a quenching from 250 °C into liquid nitrogen, while P6C<sub>F</sub>S and P6C<sub>F</sub>SO become completely amorphous after this quenching

process and do not crystallize when heated at 10 °C/min. The crystallization rate of these polymers follows the sequence of P6C<sub>F</sub>Non > P6C<sub>F</sub>Ox > P6C<sub>F</sub>K > P6C<sub>F</sub>SO ~ P6C<sub>F</sub>S. This order is correlated with the bond angles of the X linkages in the polymers. All these polymers have very high solubility in common organic solvents such as acetone, tetrahydrofuran, DMAc, and dimethylsulfoxide. Casting the tetrahydrofuran solutions of these polymers on glass slides produces uniform films. They showed much higher water contact angles than that of the non-fluorinated or partially fluorinated analogues. With the polarity of the X linkages decreased in the sequence of SO, Ox, K, S, and Non, the contact angle increases from 82° to 95°, 102°, 109°, and 110°. The last two values are close to that of Teflon (112°), indicating high hydrophobicities of the polymers.

**Acknowledgment.** This manuscript is NRC Publication Number 49127. Jianfu Ding thanks Jacques Roovers for fruitful discussions and his suggestions.

### References and Notes

- (1) (a) Yang, Z.-Y.; Feiring, A. E.; Smart, B. E. *J. Am. Chem. Soc.*, **1994**, *116*, 4135–4136. (b) *Fluoropolymers* Hougham, H., Cassidy, P. E., Johns, K., Davidson, T., Eds.; Kluwer Academic/Plenum: New York, 1999. (c) Grainger, D. W.; Stewart, C. W. In *Fluorinated Surfaces, Coatings and Films*; Castner, D. G., Grainger, D. W., Eds.; American Chemical Society: Washington, DC, 2001; pp 1–14. (d) Zhou, M. *Opt. Eng.* **2002**, *47*, 1631–1643. (e) Hickner, M. A.; Ghassemi, H.; Kim, Y. S.; Einsla, B. R.; McGrath, J. E. *Chem. Rev.* **2004**, *104*, 4587–4612. (f) Souzy, R.; Ameduri, B. *Prog. Polym. Sci.* **2005**, *30*, 644–687. (g) Kostov, G.; Ameduri, B.; Sergeeva, T.; Dolbier, W. R., Jr.; Winter, R.; Gard, G. L. *Macromolecules* **2005**, *38*, 8316–8326. (h) Feiring, A. E.; Crawford, M. K.; Farnham, W. B.; Feldman, J.; French, R. H.; Junk, C. P.; Leffew, K. W.; Petrov, V. A.; Qiu, W.; Schadt, F. L., III.; Tran, H. V.; Zumsteg, F. C. *Macromolecules* **2006**, *39*, 3252–3261.
- (2) (a) Lee, H.-J.; Lee, M.-H.; Oh, M.-C.; Ahn, J.-H.; Han, S. G. *J. Polym. Sci., Part A: Polym. Chem.* **1999**, *37*, 2355–2361. (b) Eldada, L.; Shacklette, L. W. *IEEE J. Sel. Topics Quantum Electron.* **2000**, *6*, 54–68. (c) Jiang, J.; Callender, C. L.; Blanchetiere, C.; Noad, J. P.; Ding, J.; Qi, Y.; Day, M. *Opt. Mater.* **2006**, *28*, 189–194.
- (3) (a) Harris J. E.; Johnson, R. N. In *Encyclopedia of Polymer Science Engineering*, Vol. 13; John Wiley & Sons: New York, 1988; pp 196–211. (b) Feiring, A. E.; Wonchoba, E. R.; Arthur, S. D. *J. Polym. Sci., Part A: Polym. Chem.* **1990**, *28*, 2809–2819. (c) Goodwin, A. A.; Mercer, F. W.; McKenzie, M. T. *Macromolecules* **1997**, *30*, 2767–2774. (d) Lee, H.-J.; Lee, M.-H.; Oh, M.-C.; Ahn, J.-H.; Han, S. G. *J. Polym. Sci., Part A: Polym. Chem.* **1999**, *37*, 2355–2361. (e) Kimura, K.; Tabuchi, Y.; Yamashita, Y.; Cassidy, P. E.; Fitch, J. W., III; Okumura, Y. *Polym. Adv. Technol.* **2000**, *11*, 757–765.
- (4) (a) Kim, J.-P.; Lee, W.-Y.; Kang, J.-W.; Kwon, S.-K.; Kim, J.-J.; Lee, J.-S. *Macromolecules* **2001**, *34*, 7817–7821. (b) Kim, J.-P.; Kang, J.-W.; Kim, J.-J.; Lee, J.-S. *Polymer* **2003**, *44*, 4189–4195. (c) Kim, J.-P.; Kang, J.-W.; Kim, J.-J.; Lee, J.-S. *J. Polym. Sci., Part A: Polym. Chem.* **2003**, *41*, 1497–1503. (d) Ghassemi, H.; McGrath, J. E.; Zawodzinski, T. A., Jr. *Polymer* **2006**, *47*, 4132–4139.
- (5) (a) Ding, J.; Liu, F.; Li, M.; Day, M.; Zhou, M. *J. Polym. Sci., Part A: Polym. Chem.* **2002**, *40*, 4205–4216. (b) Liu, F.; Ding, J.; Li, M.; Day, M.; Robertson, G.; Zhou, M. *Macromol. Rapid Commun.* **2002**, *23*, 844–848. (c) Ding, J.; Day, M.; Robertson, G. P.; Roovers, J. *Macromol. Chem. Phys.* **2004**, *205*, 1070–1079. (d) Ding, J.; Qi, Y.; Day, M.; Jiang, J.; Callender, C. L. *Macromol. Chem. Phys.* **2005**, *206*, 2396–2400. (e) Qi, Y.; Ding, J.; Day, M.; Jiang, J.; Callender, C. L. *Chem. Mater.* **2005**, *17*, 676–682. (f) Ding, J.; Day, M. *Macromolecules* **2006**, *39*, 6054–6062.
- (6) (a) Johncock, P.; Hewins, M. A. H.; Cunliffe, A. V. *J. Polym. Sci., Polym. Chem.* **1976**, *14*, 365–378. (b) Feiring, A. E.; Wonchoba, E. R. *J. Polym. Sci., Part A: Polym. Chem.* **1994**, *32*, 389–392. (c) Miyatake, K.; Oyaizu, K.; Tsuchida, E.; Hay, A. S. *Macromolecules* **2001**, *34*, 2065–2071.
- (7) Kim, T. K.; Kim, J. H. (Kim, M.-H., assignee) Fluorinated polyethers having perfluorinated aliphatic group and optical waveguide using the same. U.S. Patent 6,946,534, Sept 20, 2005.
- (8) Ding, J.; Du, X.; Day, M.; Jiang, J.; Callender, C. L.; Stupak, J. *Macromolecules* **2007**, *40*, 3145–3153.
- (9) Gassman, P. G.; Lumb, J. T.; Zalar, F. V. *J. Am. Chem. Soc.* **1967**, *89*, 946–952.
- (10) (a) Davies, D. G.; Derenberg, M.; Hodge, P. *J. Chem. Soc. C: Organic* **1971**, 455–460. (b) March, J.; Plankl, W. *J. Chem. Soc., Perkin Trans. I* **1977**, 460–464.
- (11) (a) Fleischer, E. B.; Sung, N.; Hawkinson, S. *J. Phys. Chem.* **1968**, *72*, 4311–4312. (b) Morley, J. O. *Int. J. Quantum Chem.* **1998**, *66*, 141–147. (c) Dingemans, T. J.; Murthy, N. S.; Samulski, E. T. *J. Phys. Chem. B* **2001**, *105*, 8845–8860.
- (12) (a) Fox, H. W.; Zisman, W. A. *J. Colloid Sci.* **1950**, *5*, 514–531. (b) Dann, J. R. *J. Colloid Interface Sci.* **1970**, *32*, 302–320. (c) Weiss, C.; Muenstedt, H. *J. Adhesion* **2002**, *78*, 507–519. (d) Kimura, K.; Nishichi, A.; Yamashita, Y. *Polym. Adv. Technol.* **2004**, *15*, 313–319. (f) Guo, J.; Resnick, P.; Efimenko, K.; Genzer, J.; DeSimone, J. M. *Ind. Eng. Chem. Res.* [Online early access]. DOI: 10/1021/ie0703179. Published online August 18, 2007. <http://pubs.acs.org/cgi-bin/asp.cgi/iecred/asp/html/ie703179.html>.
- (13) (a) Nishino, T.; Meguro, M.; Nakamae, K.; Matsushita, M.; Ueda, Y. *Langmuir* **1999**, *15*, 4321–4323. (b) Acatay, K.; Simsek, E.; Owyang, C.; Menciloglu, Y. Z. *Angew. Chem., Int. Ed.* **2004**, *43*, 5210–5213. (c) Li, X.-M.; Reinhoudt, D.; Crego-Calama, M. *Chem. Soc. Rev.* **2007**, *36*, 1350–1368.

MA071669U